16

Londono, John, Juan M. Lorenzo, and Victor Ramirez, 2012, Lithospheric flexure and related base-level stratigraphic cycles in continental foreland basins: An example from the Putumayo Basin, Northern Andes, *in* D. Gao, ed., Tectonics and sedimentation: Implications for petroleum systems: AAPG Memoir 100, p. 357–375.

Lithospheric Flexure and Related Base-level Stratigraphic Cycles in Continental Foreland Basins: An Example from the Putumayo Basin, Northern Andes

John Londono[1]

Shell Exploration and Production, 150 North Dairy Ashford, Houston, Texas, 77079, U.S.A. (e-mail: j.londono@shell.com)

Juan M. Lorenzo

Department of Geology and Geophysics, Louisiana State University, E235 Howe-Russell Complex, Baton Rouge, Louisiana, 70803, U.S.A. (e-mail: gllore@lsu.com)

Victor Ramirez

Empresa Colombiana de Petroleos, Ecopetrol, Calle 37 No. 8-43, Piso 8, Bogota, Colombia, U.S.A. (e-mail: victor.ramirez@ecopetrol.com.co)

ABSTRACT

First-order lithospheric flexure, in response to discrete tectonic and sedimentary loads, controls basin-scale, base-level cycles in upstream deposits of retroarc continental foreland basins, in the absence of dynamic topography. A depositional sequence in this type of basin may be defined as a sedimentary succession formed during the adjustment of the fluvial systems to the equilibrium stage at or near base level. This sequence spans two accommodation episodes. The initial episode with high rates of subsidence corresponds to a thrust-loading period near the hinterland end of the elastic plate and may be identified by regional seismic-reflector onlap shifts from the foreland toward the hinterland. The second episode deepens and enhances the foreland flexure under the weight of the new sediment and may be identified seismically by a continuous onlap migration toward the foreland. A depositional cycle ends either when a period of nondeposition dominates the basin because the fluvial system attains the graded stage at or near-base level or with the reactivation of thrusting activity, initiating a new cycle. Base level appears to control the top of the sedimentation boundary, but can adjust passively, during vertical movements caused by the regional isostatic compensation of the

[1] *Previous address*: Department of Geology and Geophysics, Louisiana State University, E235 Howe-Russell Complex, Baton Rouge, Louisiana, 70803, U.S.A.

DOI:10.1306/13351561M1003537

elastic plate. Regional paraconformities appear to represent periods of equilibrium of the depositional profile when the fluvial systems reach a graded stage and total tectonic quiescence.

Seismic and well data from the northern-Andes, continental retroarc Putumayo foreland basin, in Colombia, are used to test the model for flexure-induced, base-level cycles. Results suggest that onlap seismic facies migrating toward the foreland predominate during sediment-controlled flexural periods (on average, ~77% of the total deflection), whereas onlap shifts from the foreland toward the hinterland mark those periods when thrust belt loads dominate flexure (on average, ~23% of the total deflection). The seismostratigraphic record exhibits as much as eight flexure-controlled Cenozoic sequences in the basin, in correspondence with an equal number of tectonic reactivation episodes. Geodynamically, the Putumayo foreland basin has been modeled to encompass a total added lithospheric deflection of as much as 450 km (279 mi) wide. During the Oligocene, the maximum subsidence rates reached approximately 150 m/m.y. (~492 ft/m.y.) and the maximum width of the effective tectonic load (a discrete part of the thrust belt) affecting the plate reached a value of approximately 30 km (~20 mi). The geometry of the effective thrust belt and the wavelength of the lithospheric deflection modeled in this article preclude the need to invoke dynamic topography as a downward force acting on the plate and creating extra accommodation in the basin. The effective elastic thickness of the plate is 30 ± 10 km (19 ± 6 mi; and has not changed apparently since the early Paleocene). Each loading event, for instance, tectonic and sediment loads, produces a corresponding forebulge whose location and dimensions change concomitant with the evolution of the basin.

INTRODUCTION

Relatively, little work has been conducted on the cause and effect link between lithospheric flexure and base-level and/or graded-profile and sedimentary sequences in continental foreland basins, despite that flexure is the main process controlling the creation of these foredeep depocenters and, consequently, their accommodation and base level (Steckler and Watts, 1978; Sclater and Christie, 1980; Beamont, 1981; Lavier and Steckler 1997; Clark and Royden, 2000; Cardozo and Jordan, 2001, Catuneanu, 2004). Tectonic uplift via thrusting at the hinterland edge of the basin increases slope and can become the primary source of sediments for fluvial systems. As a result, river competence and sediment load also increases, although discussion still remains regarding the synchronicity between uplift and deposition of resultant conglomeratic units (Schumm, 1993; Horton, 2004). On average, rates of tectonic uplifting can be eight times higher than average denudation rates so that a time lag between uplift and denudation is expected between these processes (Lawrence and Williams, 1987; Blair and McPherson, 1994).

Although the regional isostatic compensation of the lithosphere to supracrustal loads has long been recognized as the primary mechanical control in foredeep development (Jordan, 1995; Cardozo and Jordan, 2001; Catuneanu, 2004; Gomez et al., 2005), most stratigraphic models in nonmarine foreland-basin sequences initially focused on the control exerted by eustasy and tectonics on accommodation in fluvial sedimentation even in areas with well-documented, fluvial-only stratigraphic settings far from marine influence (Posamentier and Vail, 1988). It is now generally accepted that the importance of sea level change diminishes in upstream deposits (Shanley and McCabe, 1994; Schumm et al., 2000; Chul, 2006). Recent studies (Milana, 1998; Plint et al., 2001; Miall, 2002; Chul, 2006; Miall, 2006) emphasize two patterns in upstream fluvial deposits: a shale-dominated-tract architecture, with isolated sand-channel bodies, representing high rates of subsidence and accommodation periods; and a channel-dominated-tract architecture representing low rates of subsidence and accommodation periods. Tectonic (subsidence and/or uplift) and climatic processes control the cycles of change in accommodation, for instance, stream discharge and sediment supply (Shanley and McCabe, 1994; Blum and Törnqvist, 2000). Experimental models developed by Allen (1978) show that slow subsidence promotes channel-belt occurrence and deposition of multistorey and multilateral sandstone sheets with relatively high ratios in the number of sandstone-mudstone beds. In contrast, abrupt subsidence permits significant deposition of fine-grained overbank deposits before the reinitiation of channel belts at a new location, resulting in sedimentary units that can be characterized by low sandstone-mudstone ratios. However, a change in the sandstone-mudstone ratio may also indicate a change in the type of stream environment, from braided (high sandstone-mudstone ratio) to meandering (low sandstone-mudstone ratio). Changes in sediment supply also predict an increase in the

sandstone-shale ratio with an increase in the amount of sediment loading (Miall, 1997). Sandstone-shale ratios are important not only because they should reflect the tectonic history of the basin in terms of subsidence rate, but also because, conversely, if the subsidence rate can be determined, via flexural analysis for example, it can be used as a predictive tool to infer reservoir facies (sandstone-mudstone ratios), channelization, and reservoir connectivity.

Accommodation in fluvial settings can be seen according to Blum and Törnqvist (2000) in terms of accumulation (the volume of space available for sediments, limited by base level) and preservation (when sediments subside below erosion levels). If subsidence does not occur, stratigraphic records might not be preserved. In addition, the concept of graded river developed by Mackin (1948) establishes that the regional slope of a stream system tends to adjust to a profile corresponding to the flow velocity required to transport the sediment load supplied to the basin, for instance, no net erosion or deposition along the regional fluvial system profile exists (Wescott, 1993; Miall, 1997; Emery and Myers, 1997). Thus, the graded stream profile has been used in fluvial systems to define the equilibrium surface that limits accomodation (Mackin, 1948; Sloss, 1962; Schumm, 1993; Emery and Myers, 1997).

In this chapter, we try to establish a causal link between the regional isostatic compensation and the regional stratigraphy of the upstream part of the continental Putumayo foreland by differentiating quantitatively, via flexural analysis, the tectonic load component of the isostatic compensation from the sediment load at different times during the evolution of the basin. We assume that the net subsidence of the basin floor balances the space for accumulation and preservation in the basin, achieved through the vertical isostatic adjustment of the lithosphere instead of the adjustment of the longitudinal stream equilibrium profile, which always tends to its graded stage. We try to reconcile three established concepts in continental foreland evolution by integrating flexure, accommodation, and graded stage into a model where base-level cycles are controlled by the regional deflection of the lithosphere. In addition, we assess the relative importance of tectonic versus sedimentary loads to the regional geometry of the basin floor and estimate the size and shape of the equivalent thrust belt load through time.

For the purpose of flexural analysis, we identify four tectonostratigraphic units bounded by hiatuses in the nondeformed seismostratigraphic records (areas that have not been affected by thrusting) and well data from the documented Putumayo retroarc foreland basin in Colombia (PRB). To use these deformed areas, it would have been necessary to reconstruct and balance these wedge-top zones, which is beyond the scope of this chapter. We note the smooth nature of the contours found in the isochore maps in Putumayo (Cordoba et al., 1997), with no indication of deformation or erosional scars. Each unit is then decompacted as a function of its porosity (Steckler and Watts, 1978). We consider that the decompacted thickness represents the minimum amount of accommodation created by flexure and needed for the accumulation of the preserved stratigraphic record. The sediment load of each decompacted unit is used in forward-model calculations using the two-dimensional (2-D) flexural theory of elastic beams under vertical loads (Hetenyi, 1946; Turcotte and Schubert, 1982). Thus, the regional compensation caused by the sediment load contained in each tectonostratigraphic unit is modeled. The difference between the decompacted thickness (a minimum value estimated for total subsidence) and the modeled flexure caused by the sediments is taken to represent the minimum flexure caused by tectonic loading. If a Coulomb wedge model for thrust belts is assumed for the tectonic load, the amount of loading can be modeled as a distributed load whose final geometry is a function of its critical taper angle. Thus, the minimum width of the thrust belt (effective load) affecting the plate can be estimated. The final geometry of the effective tectonic load will indicate the need to invoke dynamic topography as an acting factor in the basin. If a reasonable thrust belt geometry is attained (i.e., it is within the range of thrust belts in similar tectonic settings around the world) and the wavelength of the first-order flexure does not exceed the order of magnitude thought to be caused by supracrustal loads only (<1000 km [621 mi]; Mitrovica et al., 1989), then sedimentary and tectonic loads would explain the deflection history of the basin. If, on the contrary, unreasonable thrust load geometries are needed to fit flexural curves and/or the first-order flexural wavelength exceeds thousands of kilometers, dynamic topography would likely need to be invoked to explain the basin deflection history and geometry.

During forward modeling, we considered that the zero contour found in the isochore maps (Cordoba et al., 1997) represents the distal limit of the primary flexural basin deflection during the given period and, therefore, the maximum width of the basin over a given elapsed time. Modern deposits along the Putumayo foothills completely fill the basin, which is now approximately 450 m [~1480 ft] above sea level, and active fluvial systems run east–west, mostly orthogonal to the modern Andes. Similarly, paleodata analyses also suggest that, during the evolution of the basin, sediment transport is mostly perpendicular to the axis of the basin and is sourced from the west (Cordoba et al., 1997). We considered that the PRB behaves as an overfilled depocenter, for instance,

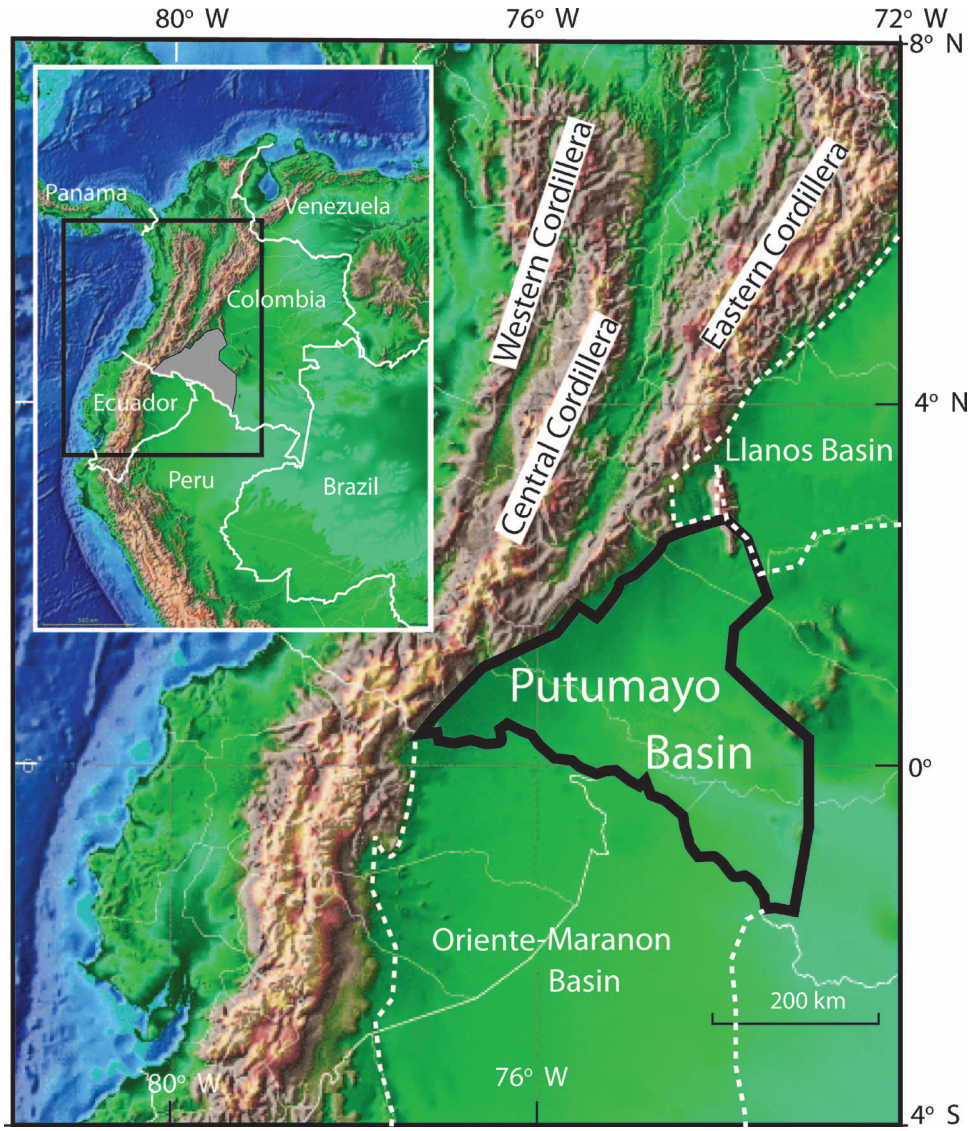

Figure 1. Putumayo retroarc foreland basin in Colombia. It extends into Ecuador and Peru with the name of Gran Cuenca de Oriente and Marañon basins, respectively. 200 km (124 mi).

the entire accommodation is full of subaerial sediments during the early foreland period. An underfilled basin would show sediment sourced from the craton in the east, and a main fluvial system running north south, parallel with the thrust belt in the present.

The Putumayo Basin, a prolific petroleum province, has the potential for 1 to 6 billion bbl of oil and 0.24 to 4.6 tcf of gas of new recoverable reserves (Higley, 2001). In Colombia, the PRB covers an area of approximately 29,900 km^2 (~11,500 mi^2) that contains 28 fields with 1.4 billion bbl of oil discovered, 0.4 billion bbl of oil produced, and 1.7 billion bbl of oil in reserves. The main reservoirs are the lower Cretaceous Caballos Formation and the upper Cretaceous Villeta and Rumiyaco formations, although reports of production from the upper Eocene Pepino Formation exist (Cordoba et al., 1997). Discoveries of commercial heavy oil in the adjacent Llanos foreland basin (Gomez et al., 2005) could indicate that the Putumayo foreland has the potential for similar accumulations, especially with traps developed in or around forebulges coevally with each loading event.

GEOLOGIC SETTING

The Putumayo foreland basin started to form in the latest Cretaceous. It is part of the so-called Sub-Andean Basin system that developed along the eastern margin of the Andes Mountains in South America (Sarmiento, 2002; Figure 1). The PRB extends from southern Colombia into Ecuador and Peru under the names of Gran Cuenca de Oriente and Marañón basins, respectively (Figure 1). The PRB has developed over the Precambrian continental crust, approximately 35 km (~20 mi)

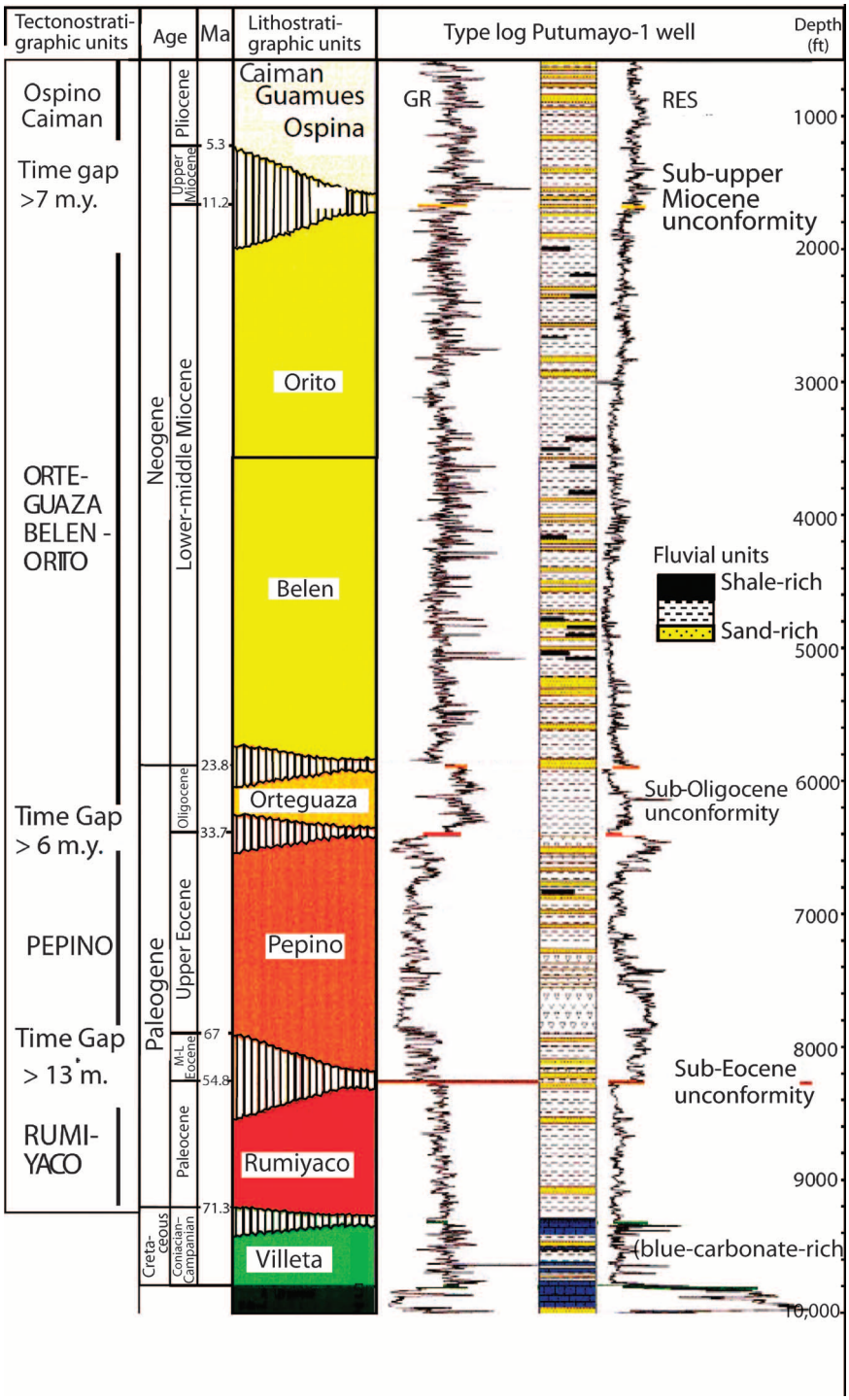

Figure 2. Stratigraphic column and well type log of the Putumayo Basin. The unconformities have been related to main uplift events during the Andes orogeny (Geotec, 1992; Cordoba et al., 1997) and identified in regional seismic lines. GR = gamma ray; RES = resistivity.

thick, adjacent to the Guyana Shield in the east (Dengo and Covey, 1993; Mora et al., 1997; Sarmiento, 2002). The transition from a back-arc basin into a foreland phase occurs during the Late Cretaceous–early Paleogene when the oceanic crust of Western Cordillera today (Figure 1) is accreted to the Central Cordillera (Hendenson, 1979; Aspden et al., 1987) and produces a thick-skin-styled thrust belt and, in the process, tectonically inverted Paleozoic normal faults along the eastern margin of the PRB (Sarmiento, 2002). The mostly continental Rumiyaco Formation (Figure 2) is deposited during this initial collisional period. The sandstone-shale average ratio in this unit has been estimated at 0.21 (Geotec, 1992).

The Tertiary tectonic history of the Putumayo Basin has been divided into three main uplift events related

to the Colombian Andean orogeny, which coincide with the dated unconformities, during the middle Eocene, Oligocene, and late Miocene (Geotec, 1992; Cordoba et al., 1997; Figure 2). The first pulse occurred during the late Paleocene–middle Eocene in response to an increase in convergence rate between the Nazca and South American plates (Daly, 1989). It has been interpreted that the continental Pepino Formation is deposited mostly in alluvial fans as a product of the continuous uplift of the Central Cordillera (Mora et al., 1997; Figure 2). The sandstone-shale average ratio in this formation has been estimated at 0.52 (Geotec, 1992). This unit is topped on the west by a regional angular unconformity that cuts the thrusts and back thrusts developed during this period. The second uplift event, caused by the collision between the Andes and the Chocó Terrane during the middle Eocene to the middle Miocene prolonged the exhumation of the Central Cordillera (Sarmiento, 2002) and is responsible for both the continental Oligocene Orteguaza Formation and the Miocene Orito and Belen formations. The sandstone-shale average ratio of this package has been estimated at 0.32 (Geotec, 1992). The third and final tectonic pulse of the foreland stage of the basin was produced by the collision of Panamá with Colombia from the late Miocene to the Holocene (Cordoba et al., 1997; Sarmiento, 2002; Figure 1). This event generated the greatest tectonic shortening and current uplift of the Central Cordillera as well as the development of the doubly vergent thrust belt that constitutes the Eastern Cordillera, in the northern part of the Putumayo Basin. The PRB area remains as an active foredeep depocenter for sediments derived from the Central Cordillera. Fluvial deposits of this period have been informally called Ospina and Caiman formations. The sandstone-shale average ratio of this package has been at 0.47 (Geotec, 1992).

DATA

Over 700 km (438 mi), 2-D, 3 s-long proprietary seismic data from Ecopetrol (Figures 3, 4) form the primary source for interpretations in this study. Composite seismic sections representative of the regional east–west geometry of the PRB (Figure 3) are assembled from more than one single seismic survey for use in flexural analysis (Londono, 2004). Over 50 proprietary well reports from Ecopetrol, containing abundant paleontologic data, are used for the isochore maps of the Rumiyaco, Pepino, and Orteguaza-Belen-Orito intervals (Figure 4; Cordoba et al., 1997). Invariably, all of these units have a characteristic wedge-shaped geometry that thins toward the foreland but shows a little change along the north–south trend, indicating a mostly symmetrical subsidence along strike.

Ecopetrol (Cordoba et al., 1997) subdivides the PRB succession into four tectonostratigraphic units (Rumiyaco, Pepino, Orteguaza-Belen-Orito, and Ospino-Caiman) based on well data that are separated by at least three regional unconformities and/or hiatuses (Figure 2). Time gaps are assessed using paleontologic records (Geotec, 1992; Cordoba et al., 1997). The seismic units between the unconformities are interpreted as seismic-stratigraphic sequences following the methodology of Vail et al. (1977). However, in the composite regional seismic-data sections, the equivalent interpreted seismic unconformable surfaces do not show any angular relationship between the overlying and underlying reflectors. No evidence of structural deformation between these units exists nor do they show any associated erosional feature (Figure 3). Bounding unconformities are not apparent in the isochore maps (Figure 4). Thus, a different mechanism is needed to explain these long-lived regional paraconformities.

We focus our interpretation within unfaulted areas that are most likely to be undisturbed by thrusting at all times and where it appears reasonable to assume that the units have preserved their original reflector geometry and thickness. Among the monotonous, and tabular, seismic facies found within the four sequences, only two types of relevant regional event terminations are recognized: continuous onlapping toward the foreland and as much as eight regional (>50 km [>31 mi]) onlap shifts toward the hinterland (Figure 3).

METHODS AND WORKFLOW

Figure 5 summarizes the basic steps we followed to develop the basin models and analysis. The four sequences are identified in the seismic data, which are depth converted using the proprietary time-to-depth curves of Geotec (1992) and Cordoba et al. (1997) based on interval velocities of more than 30 wells. Interval velocity ranges between 7500 ft/s (2287 m/s) and 18000 ft/s (5488 m/s; Geotec, 1992). The thickness of each unit was calculated and compared against the isochore maps from Ecopetrol (Geotec, 1992; Cordoba et al., 1997) to check for consistency between the two data sets. The estimated difference between the seismic data and the maps is approximately 10% on average. Each sequence, modeled in a composite profile along the seismic lines and extended to the edge of the basin using the isochore maps, is decompacted as a function of its porosity (Watts, 2001; Table 1), assuming a decompacted original porosity of 49% and an exponential constant of 0.27/km (Cordoba et al., 1997). Although

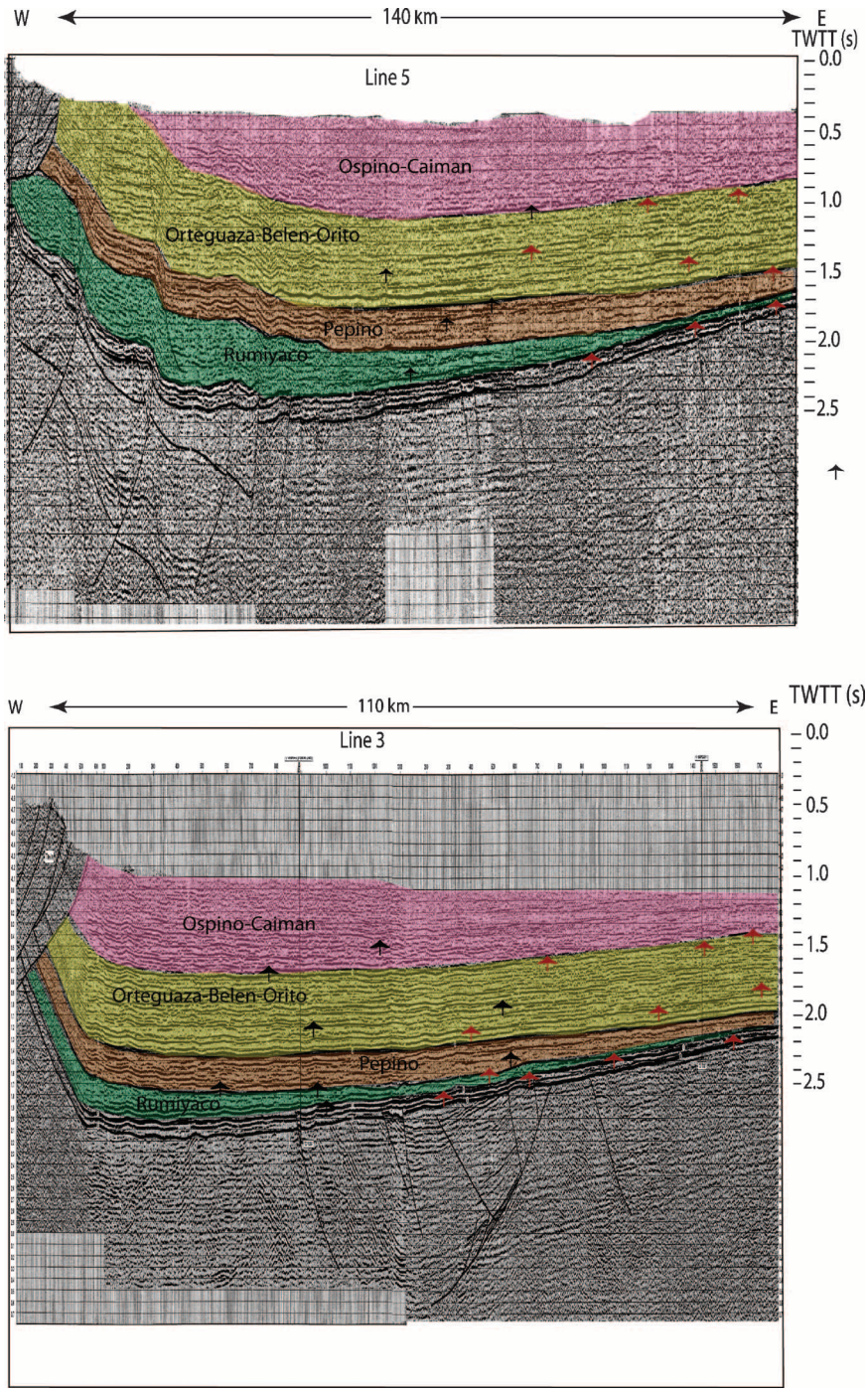

Figure 3. Composite seismic lines 3 (north) and 5 (south; line locations are shown in Figure 4). Color indicates tectonostratigraphic units, as used in this study, bounded by unconformities (thicker lines represent strong events in seismic lines). We interpret foreland onlap toward the east (red arrows) and hinterland onlap shift toward the west (black arrows). The maximum onlap shift within the data boundaries reaches approximately 75 km (~45 mi); as much as eight of these events are found in the foreland sequences (seismic line 3). TWTT = two-way traveltime. 110 km (68.3 mi); 140 km (87 mi).

Jimenez (1997) estimated a 15% tectonic shortening in the Putumayo foothills, thickness values from isochore maps are assumed to be the maximum possible values for each sequence (i.e., maximum flexure when decompacted). The error in thickness when it is not adjusted by tectonic shortening is estimated between 10 and 13% but is considered acceptable, given the unknown nature of the continuation of the thrust belt below the Central Cordillera in the area. Thus, thickness reduction by compaction is estimated in the 15 to 35% range. The parameters used for flexural modeling are summarized in Table 1.

The implementation of flexural modeling assumes that the top of the decompacted continental sequence is originally at base level and that its thickness represents the accommodation of the basin at depositional time, created by the combined effect of tectonic and sedimentary loads deflecting the lithosphere. The amount

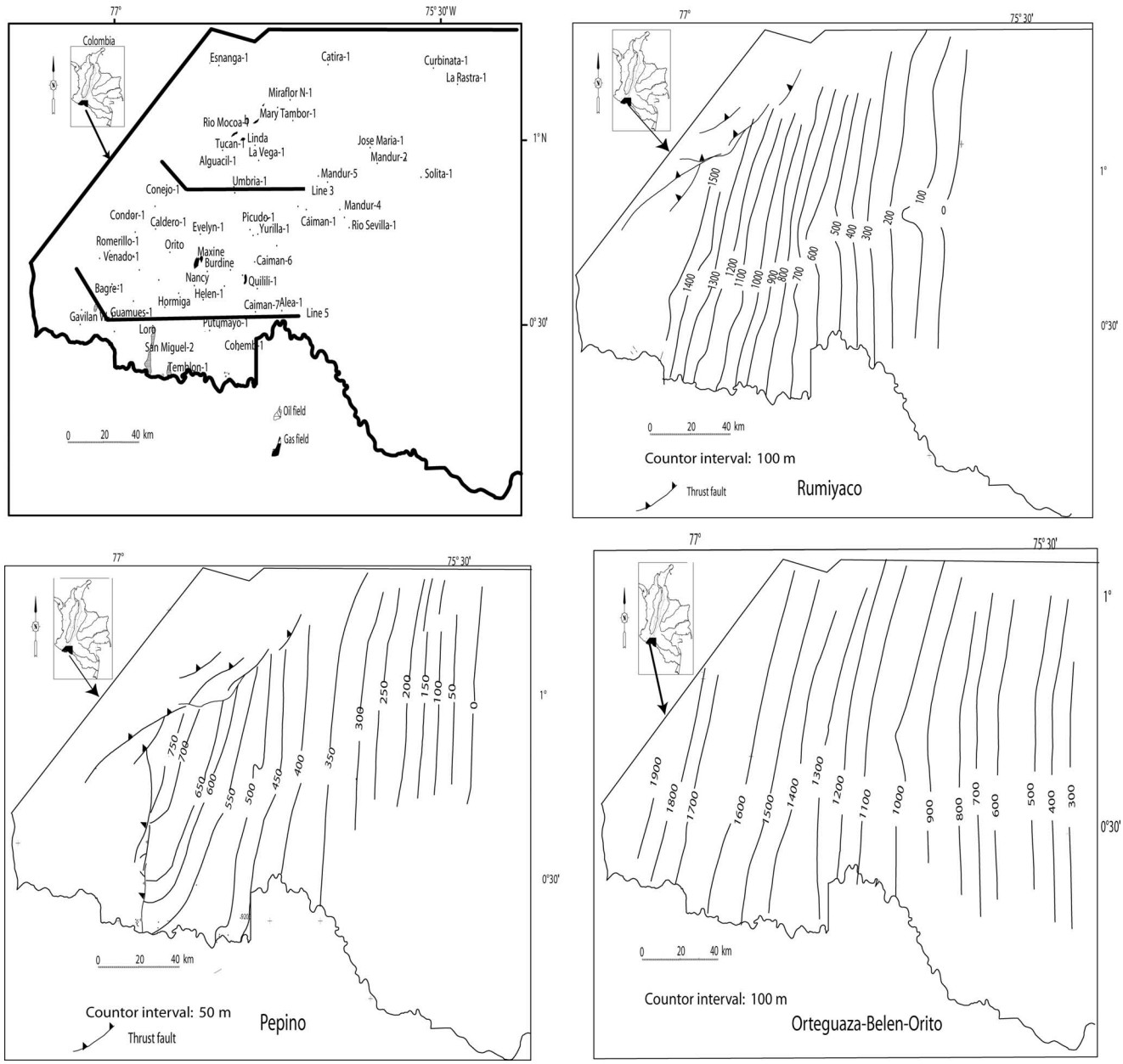

Figure 4. Well location and isochore maps showing wedge-like geometries of stratigraphic units (modified from Cordoba et al., 1997). No erosional scars of regional extent are evident in the maps. Values of these isochore maps were used to constrain flexural modeling. 40 km (24.8 mi).

of flexural subsidence caused by sediment loading is then calculated with a range of effective elastic thickness (10–100 km [6.21–62.1 mi]). The sediment load is discretized into individual linear loads (10-km [6-mi]–wide rectangles) whose heights are a function of the decompacted thickness change along the seismic profiles and isochore maps (Figure 5).The contribution to the overall deflection from each individual rectangle is integrated assuming linear superposition (Hetenyi, 1946). The calculated amount of deflection caused by the decompacted load is subtracted from the original thickness of the decompacted sequence. If the decompacted thickness exceeds the calculated deflection caused by the decompacted sedimentary load, then the residual deflection is taken to represent the minimum accommodation created by thrust-wedge loads at the time just before deposition, this residual flexure is explained by a tectonic load. However, if the decompacted thickness is smaller than the calculated deflection caused by the decompacted load, we assume that no tectonic loading is needed to create the minimum accommodation for the sedimentary sequence.

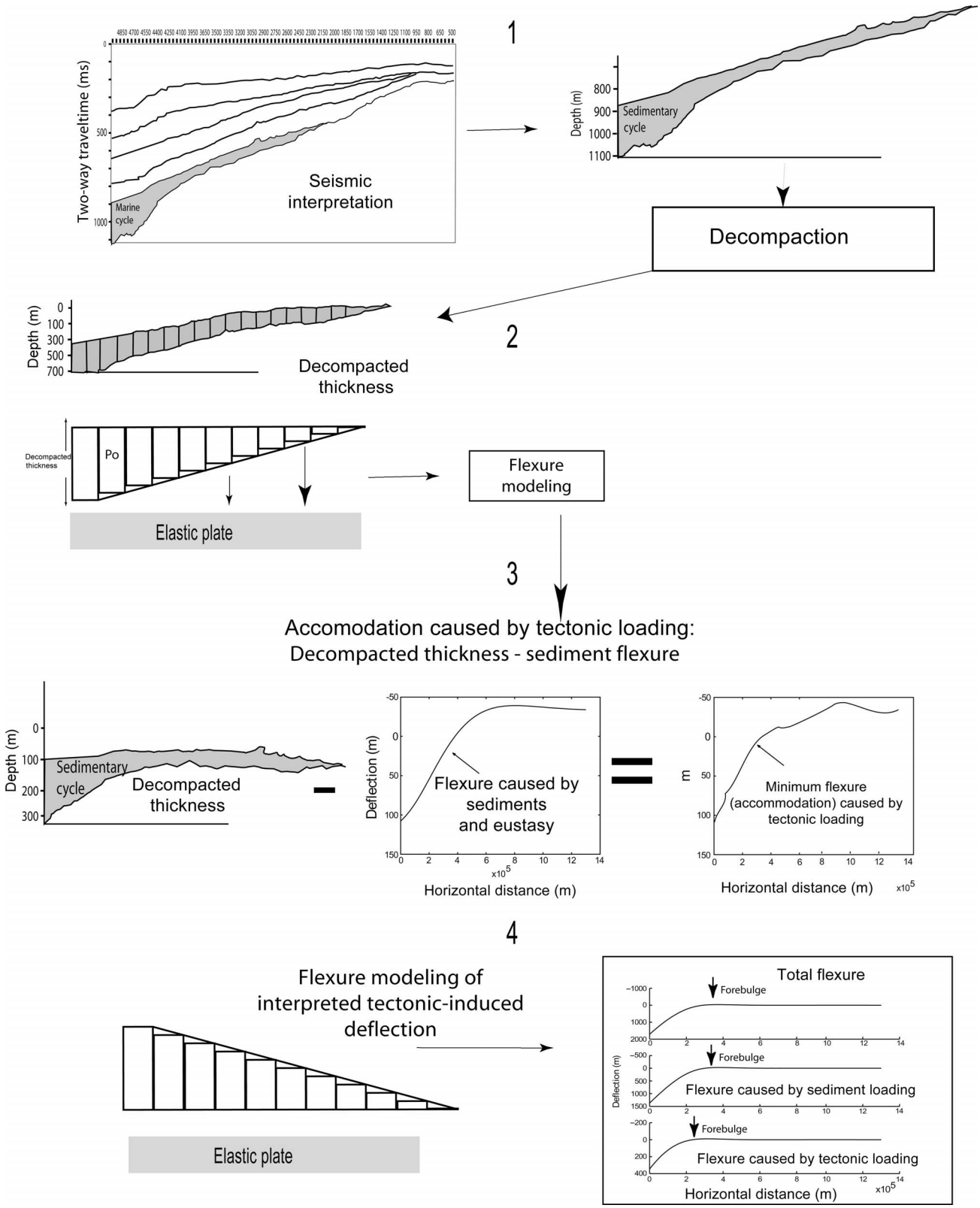

Figure 5. Workflow for flexural analysis. (1) Seismic interpretation and identification of chronostratigraphic units followed by decompaction as a function of porosity. (2) Flexural modeling of sedimentary load. (3) Residual flexure is estimated (represents tectonic-related flexure). (4) Flexural modeling of tectonic wedge. This is an iterative modeling because effective elastic thickness also needs to be modeled. Results show the tectonic, and sedimentary flexure, forebulge location and geometry, the effective elastic thickness, and the estimated width of tectonic wedge. Po = vertical load.

Table 1. Geodynamic constants*

Constant	Symbol	Value	Units
Gravity acceleration	g	9.8	m/s^2
Water density	ρ_w	1035	kg/m^3
Sediment density	ρ_s	1800–1900	kg/m^3
Density of tectonic wedge	ρ_{sw}	2500	kg/m^3
Density mantle	ρ_m	3300	kg/m^3
Young's modulus	E	5×10^{11}	Pa
Poisson's ratio	ν	0.25	
Porosity exponent	c	0.27	1/km

*Porosity exponent taken from Cordoba et al. (1997).

This residual, tectonically induced deflection is then forward modeled iteratively to determine the geometry of the best-fitting tectonic load and an effective elastic thickness comparable to that corresponding to the previously modeled sedimentary package (i.e., we assume that no effective elastic thickness changes during the elapsed time between the onset of tectonic loading and the end of the sedimentary cycle; Figure 5). During modeling, the hinterland end of the tectonic wedge coincides with the edge of the semi-infinite elastic plate in our flexural models, for instance, we assumed that this is the end of the effective load or effective tectonic wedge, although this end does not coincide with the geologic thrust belt hinterland limit that may extend farther toward the arc but has no significant effect on the flexing plate (Watts, 2001). We can estimate the geometry of the tectonic load if we assume that it behaves as a Coulomb wedge, with a critical taper angle that remains constant during thrust belt evolution (Davis et al., 1983). Then, the dimensions of the wedge such as its width and height can be determined. We divided the wedge body along the dip into discrete 1 km (0.6 mi) wide rectangles whose heights are a function of the thrust belt taper angle taken from regional cross sections (Figure 6). The taper angle used during modeling was 7°. It was the average of the cross sections found in published and proprietary articles (Portilla et al., 1993; Geotec, 1992; Dengo and Covey, 1993; Balkwill et al., 1995; Cordoba et al., 1997; Jimenez, 1997).

The computational routine used for forward modeling is developed using MATLAB® (Londono, 2004). The equilibrium equation, $D\frac{d^4w}{dx^4} + (\rho_m - \rho_{if})gw = q(x)$ (Turcotte and Schubert, 1982), is used to calculate the deflection of infinite and semi-infinite elastic beams under vertical loads (where D is flexural rigidity, $w(x)$ is deflection, x is the horizontal distance from plate end, ρ_m is density mantle, ρ_f is the density of basin-filling sedimentary rocks, g is gravity, and $q(x)$ is the vertical load; Table 1). We implement the solution developed by Hetenyi (1946) for semi-infinite beams in which several linear loads load the beam from the end ($x = 0$) inward so that they represent the distributed tectonic and sedimentary loads flexing the plate (Figure 6):

$$\begin{aligned} w(x) = \frac{q(x)}{2\alpha(\rho_m - \rho_{if})g}\,[&\{e^{-x/\alpha}(\cos\frac{x}{\alpha} - \sin\frac{x}{\alpha}) \\ &+ 2e^{-x/\alpha}(\cos\frac{x}{\alpha})\}\{e^{-x/\alpha}(\cos\frac{x}{\alpha} + \sin\frac{x}{\alpha})\} \\ &- [2\{e^{-x/\alpha}(\cos\frac{x}{\alpha} - \sin\frac{x}{\alpha}) + e^{-x/\alpha}(\cos\frac{x}{\alpha})\} \\ &\times \{e^{-x/\alpha}(\sin\frac{x}{\alpha})\}] + e^{-x/\alpha}(\cos\frac{x}{\alpha} + \sin\frac{x}{\alpha})] \end{aligned} \quad (1)$$

Where α is the flexural parameter (sensu Turcotte and Schubert, 1982). Geodynamic constants such as the

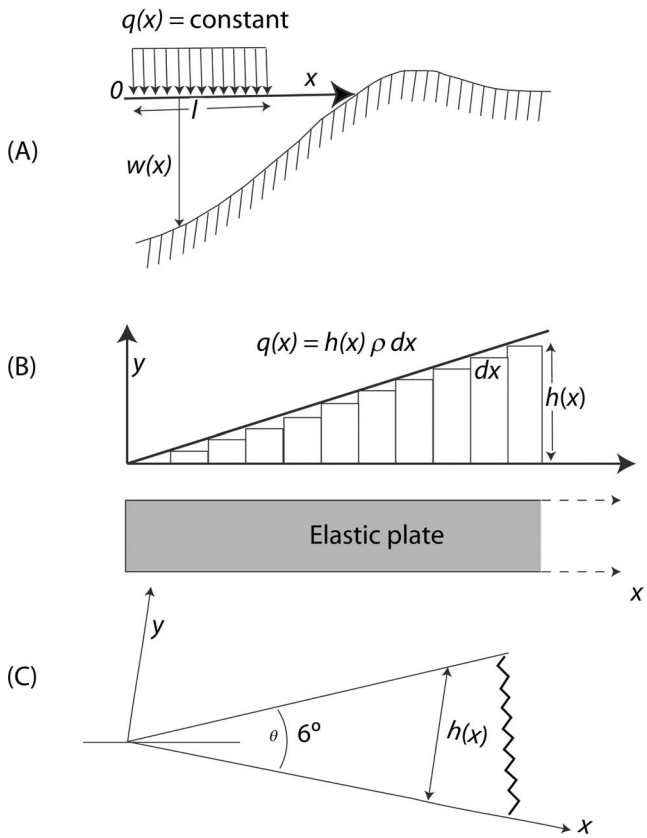

Figure 6. Flexural modeling of the tectonic load. (A) The tectonically induced deflection is forward modeled iteratively to best match the geometry of the tectonic load and the effective elastic thickness. (B) During modeling, the hinterland end of the tectonic wedge coincides with the edge of the semiinfinite elastic plate in our flexural models. We divide the wedge body into discrete, 1 km (1 mi) long rectangles whose heights are a function of the thrust belt taper angle (B, C), taken from regional cross sections.

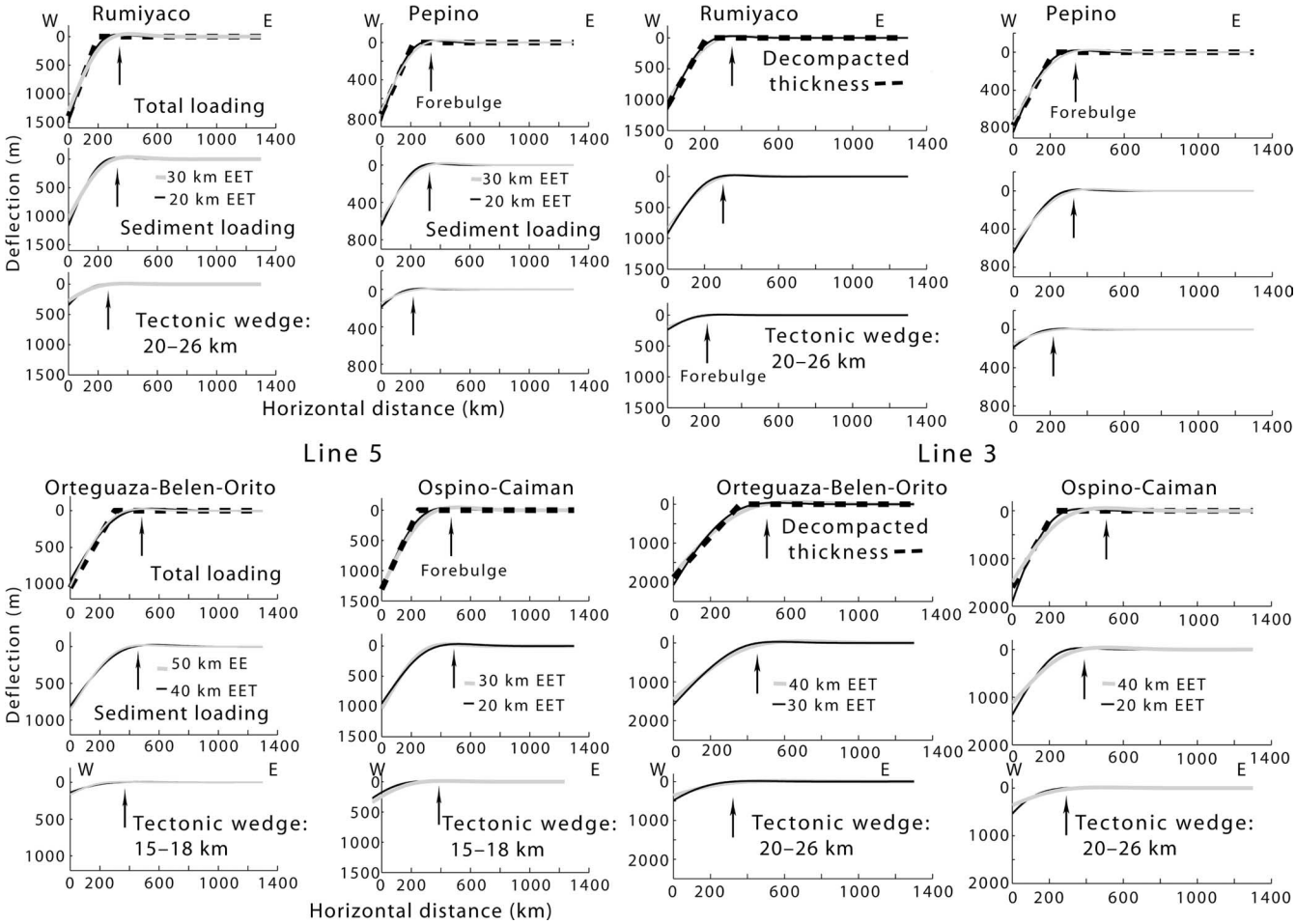

Figure 7. Flexural modeling results for composite seismic lines 5 (left) and 3 (right). For each tectonostratigraphic unit, the upper panel represents total flexure, the middle panel represents sedimentary flexure, and the lower panel represents tectonic flexure. Dashed lines represent the decompacted thickness of tectonostratigraphic units; gray lines represent total flexure; and solid black lines represent tectonic and sedimentary flexures. Note how the location of the forebulge changes concordantly with the evolving geometry of the sedimentary cover and thrust belt. EET = effective elastic thickness.

Poisson's ratio and Young's modulus (which constrains the flexural rigidity (D) and/or effective elastic thickness of the plate) are shown in Table 1. For an ideal elastic plate, the flexural subsidence is treated as occurring instantaneously with each loading phase.

FLEXURAL MODELING RESULTS

Flexural modeling using a semi-infinite homogeneous elastic plate is able to reproduce the subsidence history of the Putumayo foreland basin (Figure 7). The elastic thickness does not change during the entire evolution of the basin but remains constant at an average of 30 ± 10 km (19 ± 6 mi). During the late Oligocene to the middle Miocene, the models along line 5 match better a slightly stronger elastic lithosphere (40 km [25 mi]). However, this value returns to 30 ± 10 km (19 ± 6 mi) in the late Miocene–Holocene. This change is difficult to explain because no reported thermal events that might have affected the crust exist. The thermal age of the crust exceeds 300 m.y. (Cordoba et al., 1997). Therefore, we favor to use an average of 30 ± 10 km (19 ± 6 mi) during the entire evolution of the basin.

The first-order flexural deflection ranges between approximately 200 km (~125 mi) because of tectonic loading during the late Eocene and approximately 400 km (~250 mi) because of sediment loading since the Miocene. According to our results, approximately 450 km (~280 mi) of elastic lithosphere were flexed during the evolution of the PRB.

The geometry of the loads has a strong control on the final geometry of the basin as is manifested in our results. The location of the forebulge changes concordantly with the evolving geometry of the sedimentary

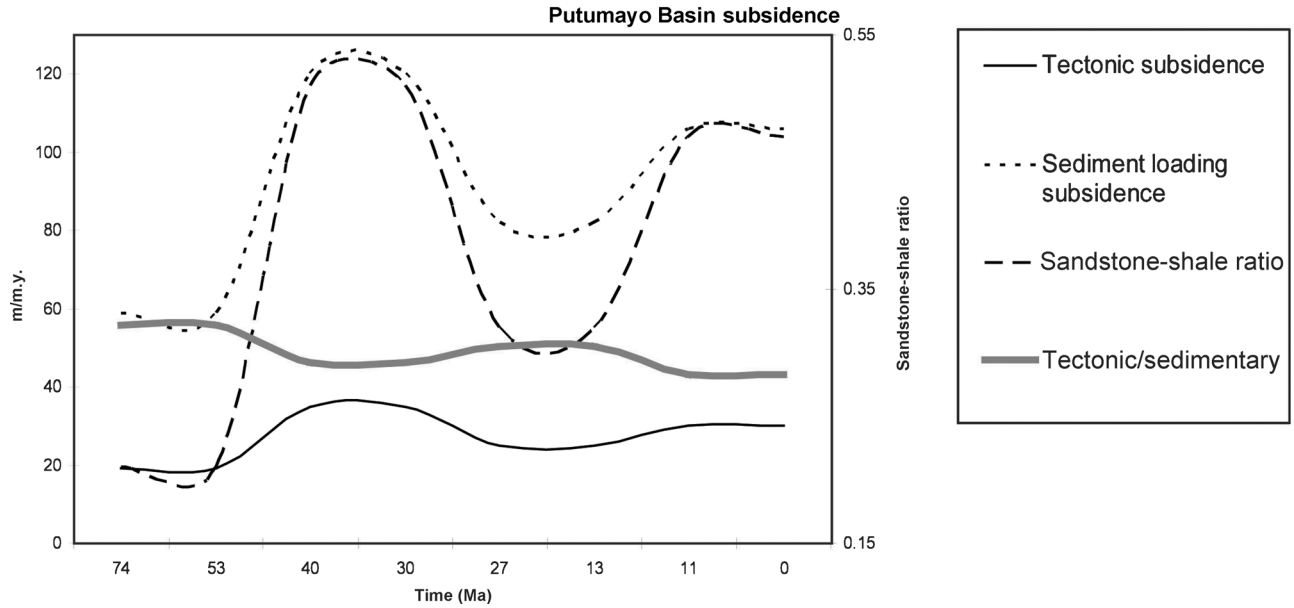

Figure 8. Summary of the history of subsidence during basin evolution. Note how sandstone-shale ratio parallels sedimentary loading.

cover and thrust belt. The geometry of the forebulge reached tens of kilometers in width but only tens of meters in height (Figure 7). Invariably, tectonic loads produce forebulges that lie closer to the hinterland and deflections that are narrower and deeper than those created by sedimentary loads. Tectonic-related forebulges during the history of the basin tend to move in the foreland direction (Figure 7).

Total foreland-sediment pileup above point-of-zero deflection reaches between 1100 ± 150 m (3608 ± 492 ft) and 1350 ± 100 m (4428 ± 328 ft; Figure 7). Tectonic deflection during the entire foreland period reaches approximately 1200 m (~3900 ft; line 3) and approximately 1000 m (~3000 ft; line 5). The difference between sediment pileup and tectonic deflection is between 150 and 250 m (492–820 ft). This difference is of the same order of magnitude as that of the present-day topography (between 500 and 250 m [1640–820 ft] in the basin), which quantitatively validates the results of the flexural model. The continental character of the basin during its foreland period indicates that it has been an area above sea level during its evolution because of sediment accumulation.

The width of the estimated effective tectonic wedge can range between 15 and 30 km (9–19 mi) for a critical taper angle of 7°. This geometry is within the parameter range of tectonic loads (thrust belts) reported in this tectonic setting around the world (Nemèok et al., 2005). The range in width values of the wedge could be a function of the uncertainty in the effective elastic thickness, which can be as high as approximately 30% in this chapter (25% for elastic thickness around the world; Burov and Diament, 1995). The height of the wedge ranges between 3 km (1.86 mi, in the Oligocene) and 1.5 km (0.93 mi, in the Eocene). Today, the Andes Mountains, contiguous to the Putumayo foreland, reach approximately 2 km (~1.24 mi) in elevation, approximately 40 km (~20 mi) from the foothills. It is noteworthy that the entire wedge is not necessarily above any datum such as sea level. Given the nature of thrust belt tectonics, it is reasonable to assume that only a part of this wedge would be subaerially exposed.

Figure 8 summarizes the flexural modeling result in terms of flexural subsidence rates at or near the deepest part of the basin. These values tend to zero at the edge of the basin (i.e., zero values in isochore maps). The Putumayo Basin reached a maximum rate of subsidence of 155 m/m.y. (508 ft/m.y.) during the late Eocene (Pepino Unit: 35 m/m.y. [114.8 ft/m.y.] resulting from tectonic loading and 120 m/m.y. [394 ft/m.y.] resulting from sediment loading) and a minimum rate of 78 m/m.y. (256 ft/m.y.) during the Paleocene: (19 m/m.y. [62 ft/m.y.] resulting from tectonic loading and 59 m/m.y. [194 ft/m.y.] resulting from sediment loading). On average, the tectonic loading subsidence is responsible for approximately 23% of the total subsidence, whereas sediment loading is responsible for the remaining 77%. The sandstone-shale ratio tends to be higher with increasing sediment-related subsidence rate: in the PRB, the highest ratio was reached during the late Eocene (Pepino Formation; Figure 8). However, it is also highest when the ratio of tectonic-related subsidence to sediment-related subsidence tends to be the lowest (Figure 8).

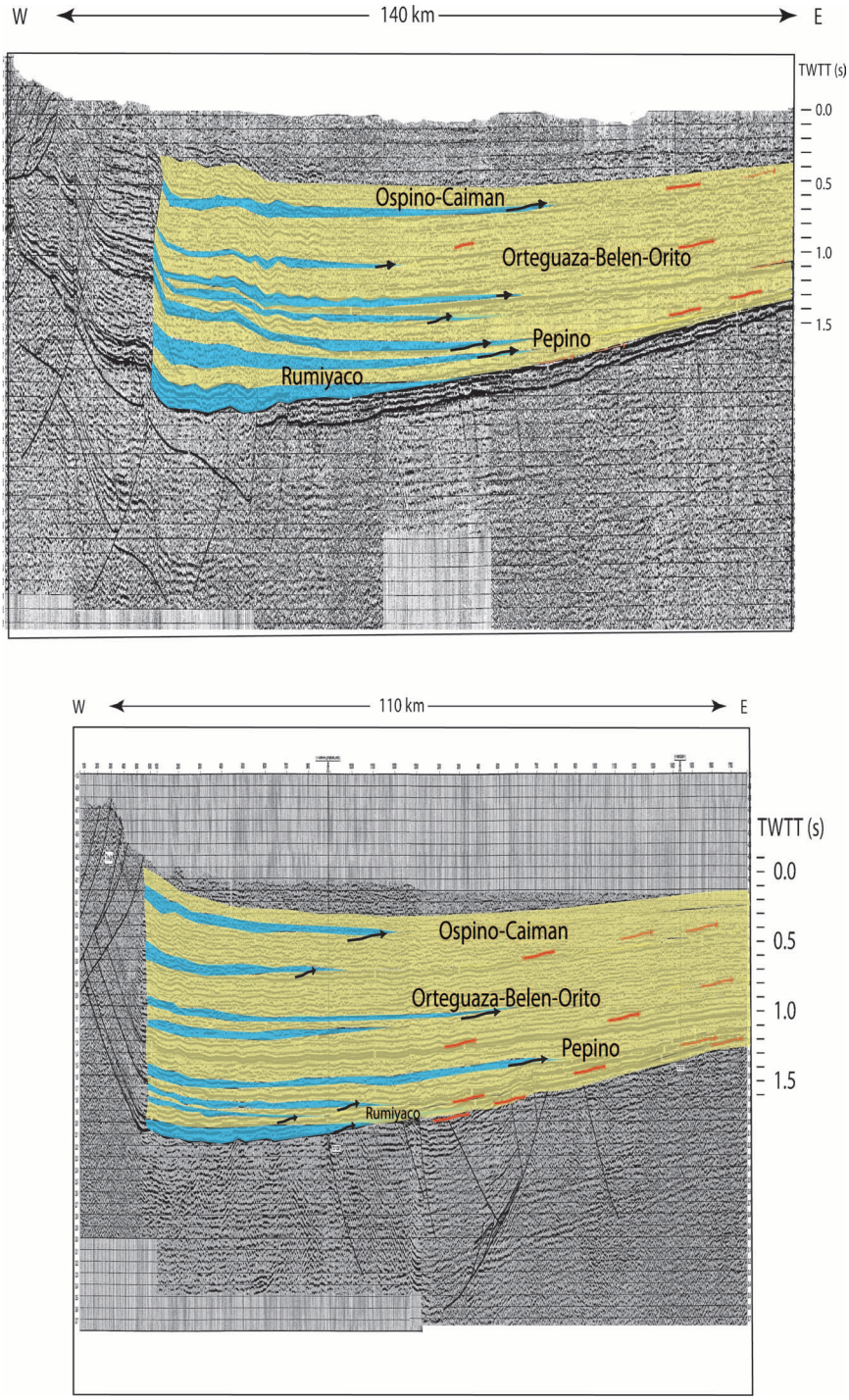

Figure 9. Seismic sections showing the results based on flexurally induced onlap and onlap-shift relationship. As much as eight regional onlap shifts (blue) are found in the seismostratigraphic data. They are interpreted renewed tectonic flexure caused by loading via thrust advancements. The onlap-shift events are overlaid by continuous foreland onlap events (yellow). TWTT = two-way traveltime. 110 km (68.3 mi); 140 km (86.9 mi).

CAUSAL LINK BETWEEN FLEXURE, ACCOMMODATION, AND BASE-LEVEL CHANGES

Despite that the seismic sequences in the Putumayo foreland exhibit a rather monotonous aggradational facies pattern, detailed seismic interpretation leads us to recognize two main reflector geometries along the entire foreland basin: a continuous onlap toward the foreland and some onlap shifts toward the hinterland (Figure 3). The maximum onlap shift, within the data boundaries, reaches approximately 75 km (~46.6 mi, during the Miocene; Figure 3). We find as much as eight of these shifts exceeding 50 km (31 mi) in the foreland sequences. Given their regional extent, these shifts indicate that accommodation is created toward the hinterland end of the depocenter (Figure 9). One

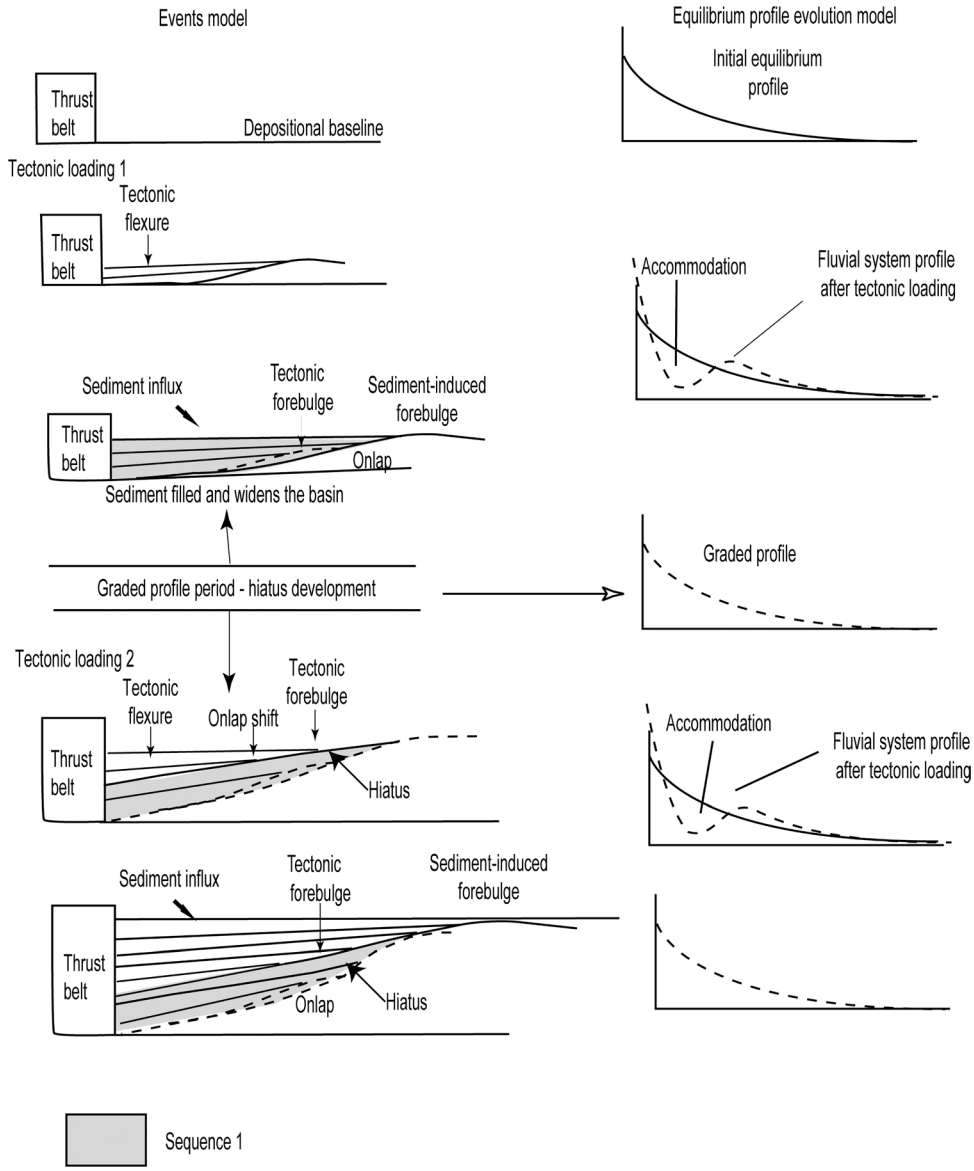

Figure 10. Foreland basin regional development model, integrating flexure, caused by tectonic and sedimentary loads, base-level and long-term hiatuses. The model initiates with a period of tectonic loading (regional hinterland onlap shifts), followed by a period of sedimentation that deepens and widens the basin resulting from sediment loading until either a new tectonic event loads the basin at the hinterland end or the fluvial system reaches the graded stage. If the latter is the case, a period of nondeposition (hiatus) follows and continues until a new loading event, via flexure, creates further accommodation.

likely cause for the deepening toward the hinterland is tectonic loading via thrust advancements. In this case, the new space for sedimentation is created through flexure of the lithosphere under these loads (Figures 3, 9). During periods of tectonic loading, the rate of creation of accommodation (flexure) is greater than the rate of sediment supply because deflection occurs instantaneously (in geologic terms). In addition, the rates of tectonic uplift may be as much as eight times those of denudation (Lawrence and Williams, 1987; Blair and McPherson, 1994). The onlap-shift events are overlaid by continuous foreland onlap events that represent continuous sedimentation without tectonic reactivation. Plate deflection tends to widen in the direction where the sediments are transported as they cover a part of the flexure created by their own weight (Figure 9).

In continental deposits, base level has been commonly considered as the limiting elevation that controls equilibrium between the processes of aggradation and degradation. This abstract definition lacks a physically equivalent boundary in the sedimentary record (Chul, 2006). We cannot always be sure whether an onlap termination coincides with the base-level elevation at that particular time of sedimentation. When a basin is flexed because of sedimentary and tectonic loads, as is the case in the Putumayo foreland basin, the depositional surface subsides continuously, creating more accommodation, although the standard base level may remain unchanged (Figure 10). Sediment aggradation proceeds up to base level and eventually tends to reach the equilibrium profile (Schumm, 1993). During the equilibrium stage, no net sediment deposition

or erosion is observed and, therefore, no stratigraphic record remains nor is an erosional scar generated (Figure 10). One possible explanation for the hiatuses reported in the Putumayo Basin is that they represent periods of an equilibrium phase, where the prevailing fluvial-system profiles are near graded stage at base level. Conversely, within this context, a sequence within the continental foreland record may be defined as a sedimentary succession formed during the adjustment of the fluvial system toward an assumed base level during an equilibrium phase (Figure 10).

In addition, and following previous studies (Milana, 1998; Chul, 2006), in the Putumayo Basin, sedimentary sequences can be divided into the following according to the subsidence regime: (1) tectonically induced high-subsidence facies, with probably low sandstone-shale ratio sediments, that are predicted to be associated with onlap shifts toward the hinterland recognizable in seismic data, and (2) sediment-loading-induced low-subsidence facies, containing probably high sandstone-shale ratios, that are predicted to be associated with continual onlap events toward the foreland bounded by onlap shifts and/or unconformities recognizable in seismic data (Figure 3). In the Putumayo Basin, some sequences contain both facies or a succession of them, suggesting that it is not necessary to reach the equilibrium stage before a change in subsidence regime occurs.

As predicted in models (Plint et al., 2001; Miall, 2002, 2006) the sandstone-shale ratio increases with the increasing amount of sediment loading (Figures 2, 8) and its ratio to tectonic load.

DISCUSSION

The results obtained in this study disagree with the current evolutionary model proposed for the Putumayo foreland basin in two fundamental aspects. First, it is unclear whether a causal link exists between tectonic episodes and resultant unconformities (Cordoba et al., 1997). It is also not clear whether the three dated tectonostratigraphic unconformities described in the Putumayo Basin (Geotec, 1992; Cordoba et al., 1997) represent single or composite uplift events followed by the sedimentation of the corresponding tectonostratigraphic unit. The interpreted unconformities show no evidence of erosion and/or structural deformation across them, and so, little evidence to explain the development of paraconformities by tectonic episodes exists. On the contrary, tectonic episodes in foreland basins have been commonly related to the abrupt deposition of coarse-grained facies (Jordan, 1995). A tectonic episode creates, necessarily, a corresponding flexural event followed by the initiation of a high-subsidence phase (Figures 7, 9, 10). The initial tectonic event is followed by a low-subsidence phase controlled mostly by sediment-induced flexure. Our model, however, indicates that these paraconformities may represent hiatuses during periods of equilibrium or graded stage of the prevailing fluvial systems and total tectonic quiescence (Figure 9). Second, we recognize as much as eight regional onlap shifts toward the hinterland (exceeding 50 km [31 mi]) that represent tectonic loading events (Figure 9). Our results support a model with more than three tectonic events to match the seven or more onlap shifts. We interpret that seven periods of thrust belt advancements are recorded in the seismostratigraphic record, and although the resolution in the data does not allow us to assess the geodynamic model for flexure for each one of these tectonic-loading related units, our model consistently explains the development of the paraconformities caused during the tectonic quiescence stage and explains the seismostratigraphic architecture found in the foreland sequences.

Figure 9 shows how at least one onlap shift or tectonic episode is interpreted during the Paleocene early in the sequence, within the limits of our seismic data. Most of the Rumiyaco Formation sequence is dominated by sediment-loading facies, represented by continuous onlap toward the foreland, before reaching the equilibrium stage that produces the succeeding 13 m.y.-time gap unconformity. However, the tectonic-related flexure is the highest at this period compared to the total subsidence and, as predicted in the models, this sequence has the lowest sandstone-shale ratio.

Within the Eocene Pepino Formation, at least two pulses of tectonic episodes can be inferred in the equivalent-age seismic data. Following the second episode, the fluvial system appears to reach the equilibrium stage that generates a hiatus of approximately 6 m.y. Also during the second period, flexural analysis suggests that the maximum subsidence rate is attained for both tectonic and sedimentary loads.

During the late Oligocene to the middle Miocene, at least three episodes of tectonic reactivation are interpreted from onlap shifts in the seismic data. These episodes occurred in the lower part of the seismic sequence: two in the lower half of the section and one toward the middle. The rates of both tectonic-related and sedimentary-related subsidence appear to be slower than for the previous Oligocene section.

Finally, since the late Miocene, at least two tectonic reactivation pulses are interpreted in the lower half of the section. Noisy data quality precludes a reliable interpretation of the upper half of the remaining seismic section. Rates of subsidence appear to increase again,

similar to those in the Oligocene, although the tectonic-related subsidence is relatively low compared to the total subsidence. As expected, a sharp increase of the sandstone-shale ratio is observed.

In our interpretation, we assume that the basin is always overfilled, for instance, the fluvial systems run transversally to the tectonic belt, which may not always be the case. We do not have evidence of an underfilled basin, in which case we expect the fluvial system to be parallel with the thrust belt, probably creating a different type of seismic facies, as described by Milana (1998).

As predicted in models (Plint et al., 2001; Miall, 2002, 2006), the sandstone-shale ratio increases with the increasing amount of sediment loading (Figures 2, 9) and its ratio to tectonic load. These results support the idea of a time gap between tectonic uplifting and denudation because they show an increasing amount of fine-grained sediments related to tectonic activity, as the amount of accommodation appears to be a lot higher than that of sediment supply. At the same time, and for the same reason, the results contradict the idea of direct temporal relationship between coarse-grained sediment and tectonic activity.

Although our models determine the maximum width and thickness of the tectonic load or the segment of the thrust belt reactivated during each studied period, we cannot establish with certainty a unique position for the load. Balance cross sections and palinspastic reconstructions extending through the mountain belt are necessary to assess the geologic position of the effective load. However, if we consider that the location of the predicted forebulges associated with each tectonic episode moves toward the foreland during the basin evolution, it is possible to infer a forward-breaking thrust sequence in the Putumayo Basin.

Flexural models predict the change of location and dimension of forebulges along the plate in response to the change in nature and magnitude of the loads throughout the basin history (DeCelles and Giles, 1996). In the Putumayo Basin, our flexural models predicted at least eight forebulges (four tectonic-related and four sedimentary-related) at different locations and with different dimensions (Figure 7). However, we interpret at least seven tectonic reactivation pulses from the seismic data. If the corresponding sediment-related forebulges are added, at least 14 forebulges should be predicted according to the foreland system models (DeCelles and Giles, 1996; DeCelles and Currie, 1996). Yet, when we consider each individual loading event, the scale of these forebulge features is subtle, only a few tens of kilometers wide and, more importantly, only tens of meters high. Distinguishing these forebulges from elevations created by autogenic processes using only stratigraphic records is an extremely difficult task (Figure 9). From the perspective of conventional and heavy oil exploration, one important implication of this assessment is that many stratigraphic traps may exist because of the larger number of tectonic pulses than identifiable in the seismic data. The location and scale of these expected traps can be predicted from flexural analysis. Exploring for hydrocarbons using a single forebulge model for the entire history of the basin could result in a costly mistake.

According to the results obtained in this study, the effective elastic thickness (30 ± 10 km [19 ± 6 mi]) does not change at a scale of 10^7 yr, similar to the results of Sinclair et al. (1991) in the Alps. No viscous-elastic relaxation seems to be necessary to explain the flexure in the Putumayo Basin. Neither the plate curvature nor the sedimentary cover, via blanketing (Lavier and Steckler, 1997), are sufficient to weaken the plate during the evolution of the basin. Cretaceous back-arc rifting processes appear to have not affected the lithosphere in Putumayo and, therefore, the thermal age of the plate is probably Precambrian to Cambrian (Sarmiento, 2002). The effective elastic thickness found in this work is similar to, or slightly lower than, the estimated thickness of the crust in the area (35–40 km [22–25 mi]; Sarmiento, 2002; Watts, 2001) during the latest episode of the Andean orogeny in Colombia during the late Miocene.

The geometry of the flexural deflection during the evolution of the PRB can be explained using tectonic and sedimentary loads only. The geometry of the modeled thrust belt (maximum width, ~30 km [~19 mi]) is within the range of similar systems around the world (Nemèok et al., 2005). In addition, because the wavelength of the first-order flexural deflection did not exceed 450 km (280 mi) at any point during the evolution of the basin, it becomes difficult to endorse dynamic topography as an acting downward force in the PRB (Mitrovica et al., 1989).

CONCLUSIONS

The regional geometry of stratigraphic sequences in retroarc foreland basins appears to be controlled primarily by the flexure of the lithosphere in response to tectonic (thrust sheets) and sediment loads. A tectonic event produces a narrow but deep depocenter, with a high subsidence rate (in relation to sediment supply) and a low sandstone-shale ratio. In the seismostratigraphic record, a tectonic loading event could be recognized by regional (tens of kilometers) onlap shifts from the foreland toward the hinterland. Conversely,

a sediment-related subsidence period (controlled mostly by the weight and dispersion of sediments) would produce a wide but relatively shallow depocenter, with a high sediment supply rate compared to the subsidence rate, and a high sandstone-shale ratio. During these periods, the flexure widens and sediments propagate toward the foreland. Seismically, these facies could be recognized by continuous foreland onlap. The end of these periods is marked in the seismostratigraphic record by the regional onlap shifts toward the hinterland that mark the initiation of a new tectonic pulse.

Retroarc foreland sequences can be seen as base-level cycles that move through several stages that include a period of tectonic reactivation, a period of sedimentary-related subsidence, and a period of graded-stage development. Base-level cycles also explain the origin of regional long-live paraconformities within a geodynamic flexural framework. A sequence, in a continental foreland setting, may be defined as a sedimentary succession formed during the adjustment of a fluvial system to the equilibrium stage at base level.

Paraconformities may represent periods of tectonic quiescence and a graded stage of the prevailing fluvial systems in the Putumayo Basin. If a sedimentary unit deposited during a period dominated by sediment loading is topped by a paraconformity, we may interpret that no tectonic reactivation immediately following its deposition (no new accommodation was made available) was observed. Without new accommodation and no new sedimentation and/or erosion, the fluvial profile would be essentially at base level and at graded stage.

In the Putumayo Basin, the highest rate of subsidence (155 m/m.y. [508 ft/m.y.]: 35 m/m.y. [114.8 ft/m.y.] because of tectonic subsidence and 120 m/m.y. [394 ft/m.y.] because of sediment-related subsidence) was attained during the Eocene.

In the Putumayo Basin, at least seven pulses of tectonic reactivation are identified in the seismostratigraphic record of the Tertiary section. These pulses are recognized as regional (>50 km [>31 mi]) onlap shifts toward the hinterland. One tectonic pulse is identified during the Paleocene (Rumiyaco Formation), at least two during the Eocene (Pepino Formation), two during the early to middle Miocene (Orteguaza-Belen-Orito Formation) and, finally, at least two since the late Miocene (Ospino-Caiman Formation). Regional unconformities and hiatuses in the Putumayo represent tectonic quiescence period where fluvial systems reached, or were near, graded stage.

The mechanical models used in this work predicted the occurrence of at least 14 forebulges, coincident with seven periods of tectonic reactivation and seven periods of sediment-controlled subsidence. The scale of these forebulges reaches tens of kilometers in width and tens of meters of height.

The subsidence history of the basin can be reproduced with an elastic semiinfinite plate, whose effective elastic thickness is 30 ± 10 km (19 ± 6 mi). Elastic plate thickness does not need to change during the evolution of the basin to match the observed data. During the history of the basin, the total deflection exceeds 5500 m (18,045 ft) vertically and over approximately 450 km (~280 mi) in width.

ACKNOWLEDGMENTS

We thank Empresa Colombiana de Petroleos (Ecopetrol) and Geotec Colombia for allowing us to use proprietary data and the Landmark Graphics Corporation for allowing us to use their software through an educational grant to the Department of Geology and Geophysics, Louisiana State University, Baton Rouge. The originally submitted manuscript was greatly benefited by the detailed constructive comments from reviewers H. Luo and D. Harry.

REFERENCES CITED

Allen, J., 1978, Studies in fluvial sedimentation: An exploratory quantitative model for the architecture of avulsion-controlled alluvial suites: Sedimentary Geology, v. 21, p. 129–147, doi:10.1016/0037-0738(78)90002-7.

Allen, P., and J. Allen, 1990, Basin analysis: Principles and applications: Oxford, United Kingdom, Blackwell Scientific Publications, 451 p.

Aspden, J. A., W. McCourt, and M. Brook, 1987, Geometrical control of subduction-related magmatism: The Mesozoic and Cenozoic plutonic history of western Colombia: Journal of the Geological Society (London), v. 144, p. 893–905, doi:10.1144/gsjgs.144.6.0893.

Balkwill, H., G. Rodriguez, F. Paredes, and J. Almeida, 1995, Northern parts of Oriente Basin, Ecuador: Reflection seismic expression of structures *in* A. Tankard, R. Soruco, and H. Welsink, eds., Petroleum basins of South America: AAPG Memoir 62, p. 559–571.

Beamont, C., 1981, Foreland basins: Geophysics Journal Research of Astronomical Society, v. 65, p. 471–498.

Blair, T., and J. McPherson, 1994, Historical adjustment by Walker River to lake-level fill over a tectonically tilted half-graben floor, Walker Lake Basin, Nevada: Sedimentary Geology, v. 92, p. 7–16, doi:10.1016/0037-0738(94)00058-1.

Blum, M. D., and T. E. Törnqvist, 2000, Fluvial responses to climate and sea level change: A review and look forward: Sedimentology, v. 47, p. 2–48, doi:10.1046/j.1365-3091.2000.00008.x.

Burov, E. B., and M. Diament, 1995, The effective elastic thickness (T_e) of continental lithosphere: What does it really mean?: Journal of Geophysical Research, v. 100, no. B3, p. 3905–3927, doi:10.1029/94JB02770.

Cardozo, N., and T. Jordan, 2001, Causes of spatially variable tectonic subsidence in the Miocene Bermejo foreland basin, Argentina: Basin Research, v. 13, p. 335–358, doi:10.1046/j.0950-091x.2001.00154.x.

Catuneanu, O., 2004, Retroarc foreland systems evolution through time: Journal of African Earth Sciences, v. 38, p. 225–242, doi:10.1016/j.jafrearsci.2004.01.004.

Chul, W., 2006, Conceptual problems and recent progress in fluvial sequence stratigraphy: Geoscience Journal, v. 10, p. 433–443, doi:10.1007/BF02910437.

Clark, M., and L. Royden, 2000, Topographic ooze, building the eastern margin of Tibet by lower crustal flow: Geology, v. 28, p. 703–706, doi:10.1130/0091-7613(2000)28<703:TOBTEM>2.0.CO;2.

Cordoba, F., E. Kairuz, J. Moros, W. Calderón, F. Buchelli, C. Guerrero, and L. Magoon, 1997, Proyecto Evaluación Regional Cuenca del Putumayo: Definición de Sistemas Petrolíferos: Ecopetrol Internal Report, 119 p.

Daly, M. C., 1989, Correlations between Nazca/Farallon plate kinematics and forearc basin evolution in Ecuador: Tectonics, v. 8, p. 769–790, doi:10.1029/TC008i004p00769.

Davis, D., J. Supper, and F. Dahlia, 1983, Mechanics of fold and thrust belts and accretionary wedges: Journal of Geophysical Research, v. 88, p. 1153–1172, doi:10.1029/JB088iB02p01153.

DeCelles, P., and B. Currie, 1996, Long-term sediment accumulation in the Middle Jurassic–early Eocene Cordilleran retroarc foreland basin system: Geology, v. 24, no. 7, p. 591–594, doi:10.1130/0091-7613(1996)024<0591:LTSAIT>2.3.CO;2.

DeCelles, P., and K. Giles, 1996, Foreland basin systems: Basin Research, v. 8, p. 105–123, doi:10.1046/j.1365-2117.1996.01491.x.

Dengo, C. A., and M. C. Covey, 1993, Structure of the Eastern Cordillera of Colombia: Implications for trap styles and regional tectonics: AAPG Bulletin, v. 77, p. 1315–1337.

Emery, D., and K. Myers, 1997, Sequence stratigraphy: Oxford, England, Blackwell Science Publications, 297 p.

Geotec, 1992, Facies distribution and tectonic setting through the Phanerozoic of Colombia: A regional synthesis combining outcrop and subsurface data presented in 17 consecutive rock-time slices: Bogotá, Colombia, Geotec Limitada, 100 p.

Gomez, E., T. E. Jordan, R. W. Allmendinger, and N. Cardozo, 2005, Development of the Colombian foreland-basin system as a consequence of diachronous exhumation of the northern Andes: Geological Society of America Bulletin, v. 117, p. 1272–1292.

Henderson, W., 1979, Cretaceous to Eocene volcanic arc activity in the Andes of northern Ecuador: Journal of the Geological Society (London), v. 136, p. 367–378.

Hetenyi, M., 1946, Beams of elastic foundation: The University of Michigan Press, 257 p.

Higley, D., 2001, The Putumayo-Oriente-Maranon Province of Colombia, Ecuador, and Peru: Mesozoic–Cenozoic and Paleozoic petroleum systems: U.S. Geological Survey Digital Data Series 63, 20 p.

Horton, B. K., K. N. Constenius, and P. G. DeCelles, 2004, Tectonic control on coarse-grained foreland-basin sequences: An example from the Cordilleran foreland basin, Utah: Geology, v. 32, p. 637–640.

Jimenez, C., 1997, Structural styles of the Andean foothills, Putumayo Basin, Colombia: Master's thesis, University of Texas at Austin, Austin, Texas, 73 p.

Jordan, T., 1995, Retroarc foreland and related basins, *in* C. Busby and R. Ingersoll, eds., Tectonics and sedimentation: Blackwell Science Publications, p. 331–362.

Lavier, L., and M. Steckler, 1997, The effect of sedimentary cover on the flexural strength of continental lithosphere: Nature, v. 389, p. 476–479, doi:10.1038/39004.

Lawrence, D., and B. Williams, 1987, Evolution of drainage systems in response to Acadian deformation: The Devonian Battery Point Formation, eastern Canada, *in* F. Ethridge, R. Flores, and M. Harvey, eds., Recent developments in fluvial sedimentology: SEPM Special Publication 39, p. 287–300.

Liu, S., and D. Nummedal, 2004, Late Cretaceous subsidence in Wyoming: Quantifying the dynamic component: Geology, v. 32, no. 5, p. 397–400, doi:10.1130/G20318.1.

Londono, J., 2004, Foreland basins: Lithospheric flexure, plate strength and regional stratigraphy: Ph.D. dissertation, Louisiana State University, Baton Rouge, Louisiana, 175 p.

Mackin, J., 1948, Concept of graded river: Geological Society of America Bulletin, v. 59, p. 463–512.

Miall, A., 1997, The geology of stratigraphic sequences: Berlin, Germany, Springer-Verlag, 433 p.

Miall, A., 2002, Architecture and sequence stratigraphy of Pleistocene fluvial systems in the Malay Basin, based on seismic time-slice analysis: AAPG Bulletin, v. 86, p. 1201–1216.

Miall, A., 2006, Reconstructing the architecture and sequence stratigraphy of the preserved fluvial record as a tool for reservoir development: A reality check: AAPG Bulletin, v. 90, p. 989–1002, doi:10.1306/02220605065.

Mora, C., M. P. Torres, and J. Escobar, 1997, Potencial generador de hidrocarburos de la Formación Chipaque y su relación estratigráfica secuencial en la zona axial de la Cordillera Oriental (Colombia): VI Simposio Bolivariano Exploración Petrolera en las Cuencas Subandinas, Cartagena, Colombia, p. 217–237.

Michal, N., S. Steven, and R. Gayer, 2005, Thrust belts: Structural architecture, thermal regimes and petroleum systems: Cambridge, United Kingdom, Cambridge University Press, 541 p.

Milana, J., 1998, Sequence stratigraphy in alluvial settings: A flume-based model with applications to outcrop seismic data: AAPG Bulletin, v. 82, p. 1736–1753.

Mitrovica, J. X., C. Beaumont, and G. T. Jarvis, 1989, Tilting of continental interiors by the dynamical effects of subduction: Tectonics, v. 8, p. 1079–1094, doi:10.1029/TC008i005p01079.

Nemcok, M., S. Schamel, and R. Gayer, 2005, Thrustbelts: structural architecture, thermal regimes and petroleum systems: Cambridge University Press, 541 p.

Plint, G., P. McCarthy, and U. Faccini, 2001, Nonmarine sequence stratigraphy, updip expression of sequence boundaries and systems tracts in a high-resolution framework, Cenomanian Dunvegan Formation, Alberta foreland basin, Canada: AAPG Bulletin, v. 85, p. 1967–2001.

Portilla, O., E. Ch. Kairuz, C. A. Y Lombo, and H. Garzón, 1993, Informe Final Proyecto Putumayo Oeste Fase III: Bogotá, Colombia, Ecopetrol, 153 p.

Posamentier, H., and P. Vail, 1988, Eustatic controls on clastic deposition II: Sequence and systems tract models, *in* C. Wilgus, B. S. Hasting, C. G. Kendall, H. W. Posamentier, C. A. Ross, and J. C. Van Wagoner, eds., Sea level changes: An integrated approach: SEPM Special Publication 42, p. 125–154.

Sarmiento, L., 2002, Mesozoic rifting and Cenozoic basin inversion history of the Eastern Cordillera, Colombian Andes: Inferences from tectonic models: Ph.D. dissertation, Vrije Universiteit, Amsterdam, The Netherlands, 295 p.

Schumm, S., 1993, River response to base-level change: Implication for sequence stratigraphy: Journal of Geology, v. 101, p. 279–294, doi:10.1086/648221.

Schumm, S., J. Dumont, and J. Holbrook, 2000, Active tectonics and alluvial rivers: Cambridge, United Kingdom, Cambridge University Press, 276 p.

Steckler, M., and A. Watts, 1978, Subsidence of an Atlantic-type continental margin off New York: Earth Planetary Sciences, v. 7, p. 1–13, doi:10.1016/0012-821X(78)90036-5.

Sclater, J. G., and P. A. F. Christie, 1980, Continental stretching: An explanation of the post–mid-Cretaceous subsidence of the central North Sea Basin: Journal of Geophysical Research, v. 85, p. 3711–3739, doi:10.1029/JB085iB07p03711.

Shanley, M., and P. McCabe, 1994, Perspectives on sequence stratigraphy of continental strata: AAPG Bulletin, v. 78, p. 654–568.

Sinclair, H., B. Coakly, P. Allen, and A. Watt, 1991, Simulation of foreland basin stratigraphy using a diffusion model of mountain belt erosion: An example from the Alps of eastern Switzerland: Tectonics, v. 10, p. 599–620, doi:10.1029/90TC02507.

Sloss, L. L., 1962, Stratigraphic models in exploration: AAPG Bulletin, v. 74, p. 93–113.

Turcotte, D., and G. Schubert, 1982, Geodynamics: Application of continuum physics to geological problems: New York, Wiley, 448 p.

Vail, P., R. Mitchum, and S. Thompson, 1977, Seismic stratigraphy and global changes of sea level: Relative changes of sea level from coastal onlap, *in* C. E. Payton, ed., Seismic stratigraphy: Applications to hydrocarbon exploration: AAPG Memoir 26, p. 63–81.

Watts, A. B., 2001, Isostasy and flexure of the lithosphere: Cambridge, United Kingdom, Cambridge University Press, 472 p.

Wescott, W., 1993, Geomorphic thresholds and complex response of fluvial systems: Some implications for sequence stratigraphy: AAPG Bulletin, v. 77, p. 1208–1218.